Title

Gremlin 1 Identifies a Skeletal Stem Cell with Bone, Cartilage, and Reticular Stromal Potential

Journal

Cell, 160(1-2)

ISSN

0092-8674

Authors

Worthley, Daniel L
Churchill, Michael
Compton, Jocelyn T
et al.

Publication Date

2015

DOI

10.1016/j.cell.2014.11.042

Peer reviewed

HHS Public Access

Author manuscript

Cell. Author manuscript; available in PMC 2016 January 15.

Published in final edited form as:

Cell. 2015 January 15; 160(0): 269–284. doi:10.1016/j.cell.2014.11.042.

Gremlin 1 Identifies a Skeletal Stem Cell with Bone, Cartilage, and Reticular Stromal Potential

A full list of authors and affiliations appears at the end of the article.

Abstract

The stem cells that maintain and repair the postnatal skeleton remain undefined. One model suggests that perisinusoidal mesenchymal stem cells (MSCs) give rise to osteoblasts, chondrocytes, marrow stromal cells, and adipocytes, although the existence of these cells has not been proven through fate-mapping experiments. We demonstrate here that expression of the bone morphogenetic protein (BMP) antagonist gremlin 1 defines a population of osteochondroreticular (OCR) stem cells in the bone marrow. OCR stem cells self-renew and generate osteoblasts, chondrocytes, and reticular marrow stromal cells, but not adipocytes. OCR stem cells are concentrated within the metaphysis of long bones not in the perisinusoidal space and are needed for bone development, bone remodeling, and fracture repair. *Grem1* expression also identifies intestinal reticular stem cells (iRSCs) that are cells of origin for the periepithelial intestinal mesenchymal sheath. *Grem1* expression identifies distinct connective tissue stem cells in both the bone (OCR stem cells) and the intestine (iRSCs).

Introduction

Long bones consist of a cortex supported by an internal framework of trabecular bone. The trabecular bone and the adjacent cartilaginous growth plates contain the cellular progenitors necessary for postnatal bone growth. The prevailing model for the development, growth, and repair of long bones proposes two phases. First, cartilage cells lay down a matrix that forms a “scaffold” for bone formation. Osteoblasts then invade this matrix and lay down the mineralized parts of bone (Kronenberg, 2003). Although this process—termed “endochondral ossification”—has been known for decades, it remains unclear whether postnatal bones are grown and repaired by osteoblasts and chondrocytes already committed to their respective lineages, or whether there are specialized multipotent cells that determine postnatal growth and repair.

The mesenchymal stem cell (MSC) model suggests that a self-renewing stem cell exists within the bone marrow that gives rise to mature osteoblasts, chondrocytes, adipocytes, and

*Correspondence: sm3252@columbia.edu (S.M.), tcw21@columbia.edu (T.C.W.).

21Co-senior authors

Supplemental Information: Supplemental Information includes Extended Experimental Procedures, five figures, one table, two data files, and one movie and can be found with this article online at http://dx.doi.org/10.1016/j.cell.2014.11.042.

Author Contributions: D.L.W., T.C.W., S.M., G.K., and F.Y.L.: study concept and design; analysis and interpretation of data; writing and revising the manuscript. All other authors contributed to the acquisition and interpretation of data and review of the manuscript.

marrow stromal cells required for skeletal development, homeostasis, and repair. A prime candidate for the endogenous MSC has been the mesenchymal cells that surround the bone marrow sinusoids (Bianco et al., 2013). Perisinusoidal mesenchymal cells are marked by nestin *(Nes)-GFP* (Méndez-Ferrer et al., 2010) and leptin receptor *(Lepr)-cre* (Ding et al., 2012; Mizoguchi et al., 2014; Zhou et al., 2014) in mice and by CD146 in humans (Sacchetti et al., 2007).

Recently, perisinusoidal mesenchymal cells expressing *Lepr* were found to include multipotent, colony-forming unit-fibroblasts (CFU-Fs) (Zhou et al., 2014). Lineage-tracing studies revealed that this perisinusoidal population also contained cells with invivo osteogenic and adipogenic potential; however, these cells gave rise to osteo-adipogenic lineages exclusively in adult animals (>8 weeks of age) and not during development or bone growth (Ding et al., 2012; Mizoguchi et al., 2014; Zhou et al., 2014). Furthermore, *Lepr*-expressing perisinusoidal cells never contributed to normal developing chondrocytes, the major cell lineage generating the cartilaginous matrix required for endochondral ossification (Ding et al., 2012; Mizoguchi et al., 2014; Zhou et al., 2014). Thus, perisinusoidal MSCs do not fulfill all of the characteristics expected of a skeletal MSC. In addition, putative MSC markers such as *Nes* (Méndez-Ferrer et al., 2010) have failed to prove that single MSCs have in vivo postnatal multipotentiality and self-renewal. Together, these data raise the prospect that another complementary postnatal skeletal stem cell may exist.

We developed an inducible *Cre* transgenic line marking a skeletal stem cell. In doing so, we discovered the osteochondroreticular (OCR) stem cell. We also provide evidence indicating that analogous connective tissue stem cells, intestinal reticular stem cells (iRSCs), exist in the small intestine.

Results

Generating a Specific Marker of Skeletal Stem Cells

To select a specific MSC marker in the bone and intestine, we considered human gene-expression arrays from bone marrow, intestine, and peritumoral mesenchyme (Delorme et al., 2009; Kosinski et al., 2007; Sneddon et al., 2006). Gremlin 1 *(Grem1)*, identified from these studies, is a secreted antagonist of bone morphogenetic protein (Bmp) -2, -4, and -7 and a VEGFR2 agonist (Hsu et al., 1998; Mitola et al., 2010). *Grem1* is important in normal skeletal and renal development and homeostasis (Canalis et al., 2012; Khokha et al., 2003; Michos et al., 2004). Furthermore, overexpression of *Grem1* interrupts normal intestinal function and has been linked to intestinal cancer (Jaeger et al., 2012).

We previously found that *Grem1* expression identified the most clonogenic fraction of marrow stromal cultures (Quante et al., 2011). In the present study, we confirmed that expression of *Grem1* was increased in undifferentiated mesenchymal cultures compared to endogenous bone marrow mesenchyme (Figures S1A–S1C available online).

To extend these findings in vivo, we generated a tamoxifen-inducible BAC transgenic *creER^T* line specific for *Grem1* expression (*Grem1-creER^T*, Figures S1D–S1F, Table S1A). The *Grem1-creER^T* BAC transgenic line was crossed to different reporters (such as *R26*-

LSL-TdTomato and *R26-LSL-ZsGreen*) and the *R26-LSL-diphtheria toxin subunit A (DTA)* line to allow lineage tracing and functional ablation of specific mesenchymal cells, respectively (See Tables S1B and S1C for summary of transgenic lines).

Grem1$^+$ Cells Are Distinct from, and More Clonogenic than, *Nes-GFP*$^+$ MSCs

Tamoxifen induction of adult *Grem1-creER*^{T}*;R26-LSL-TdTomato* mice (Figure 1A) resulted in recombination in and expression of the TdTomato reporter (red fluorescent protein) in a rare and exclusively mesenchymal population of bone marrow cells (0.0025% of all single, live, nucleated cells after collagenase digestion [95% confidence interval (CI) 0.0022–0.0028]). In this experiment and elsewhere in the paper, we defined skeletal mesenchymeastriple negative for CD45$^-$Ter-119$^-$CD31$^-$ in enzymatically digested bone and bone marrow cells. CD45 characterizes most hematopoietic cells with the exception of maturing erythroid cells, which are marked by Ter-119. CD31 was used to exclude endothelial cells (Park et al., 2012) (Table S1D). The CD45-negative, Ter-119-negative, and CD31-negative fraction of bone marrow defines the nonendothelial, nonhematopoietic compartment that contains putative skeletal stem cells. Many *Grem1-creER*$^{T+}$ cells, identified by a recombined fluorescent reporter gene shortly after tamoxifen administration (hereafter referred to as *Grem1*$^+$ cells), were immediately adjacent to the growth plate and trabecular bone (Figures 1B, 1C, and 5B).

To determine the overlap between *Grem1*$^+$ and other reported CFU-F populations, we crossed *Grem1-creER*^{T} to *Nes-GFP*; *R26-LSL-TdTomato* (*Grem1*$^+$ cells and their progeny were red, and *Nes-GFP*-expressing cells were green) and to *Acta2-RFP;R26-LSL-ZsGreen* (*Grem1*$^+$ cells and their progeny were green, and *Acta2-RFP*-expressing cells were red) (Grcevic et al., 2012; Méndez-Ferrer et al., 2010). Adult *Grem1*$^+$ cells did not express *Nes-GFP* (Figures 1B and 1D), and only a minority of *Grem1*$^+$ cells expressed *Acta2-RFP* (mean 5.9% of *Grem1*$^+$ were *Acta2*$^+$; Figure S2A). The *Grem1*$^+$ population was more clonogenic than *Nes-GFP* or *Acta2-RFP* cells, even after depletion of contaminating nonmesenchymal lineages (Figures 1D–1G and S2B). *Grem1*$^+$ CFU-Fs did not initially express *Acta2-RFP*, but during culture, the *Grem1*$^+$ progeny differentiated into *Acta2-RFP*-expressing myofibroblasts (these cells were yellow, expressing both *ZsGreen* and *Acta2-RFP;* Figure S2C). Importantly, the proportion of CFU-Fs was diminished within the *Grem1*$^+$ descendants expressing *Acta2-RFP*, suggesting that *Acta2* expression marks a more differentiated cell less capable of clonogenic growth (Figure S2D). *Grem1*$^+$ cells, however, never gave rise to *Nes-GFP*-expressing cells, either in adherent culture or in vivo (10 months tracing after adult tamoxifen induction of *Grem1-creER*^{T}*;R26-LSL-TdTomato;Nes-GFP* mice; Figure S2E).

For the clonal differentiation experiments (Figure 1), adult *Grem1-creER*^{T}*;R26-LSL-ZsGreen;Acta2-RFP* and *Grem1-creER*^{T}*;R26-LSL-TdTomato* mice were administered tamoxifen by oral gavage at 6–8 weeks of age. Bones were processed as described (see Experimental Procedures), and the fluorescent *Grem1*$^+$ cells were sorted by fluorescence-activated cell sorting (FACS) and plated at clonal density < 2,500 cells/10 cm dish. Clones (i.e., isolated clusters of > 50 cells at 10–14 days) were harvested using a cloning cylinder and expanded into individual wells for differentiation. We evaluated 19 clones after in vitro

differentiation. Single clones gave rise to osteoblasts (defined by alizarin red [Figure 1H] or alkaline phosphatase staining in 84% of clones, [Figures S2F and S2G]), chondrocytes (100% ofclones confirmed by toluidine blue staining), and myofibroblasts on the basis of coexpression of the *Acta2-RFP* transgene (100%, Figures 1H–1J). In contrast, the *Grem1*$^+$ cell-derived clones showed little capacity for adipocytic differentiation (defined by oil red staining, Figure 1K, 0 of 19 single clones). Polyclonal cultures from sorted *Grem1*$^+$ cells also failed to differentiate into adipocytes.

A substantial proportion (40%) of *Grem1*$^+$ cells, in addition to being triple negative for CD45$^-$Ter-119$^-$CD31$^-$, were also positive for CD105, a well-established marker of bone marrow CFU-Fs (Park et al., 2012). In contrast, less than 2% of the Grem1-negative cells were CD45$^-$CD31$^-$Ter-119$^-$CD105$^+$. *Grem1*$^+$ cells, however, expressed lower levels of CD140a and Sca-1 (Figures 2A–2F). The *Grem1*$^+$ population was enriched for CD45$^-$CD31$^-$Ter-119$^-$CD105$^+$ cells, a subpopulation previously reported to contain all mouse bone marrow CFU-Fs (Park et al., 2012). It followed that *Grem1*$^+$ cells were also enriched for CFU-Fs compared to *Grem1*-negative fractions (Data S1A and S1B). It is worth noting that we used standard adherent cell culture conditions (aMEM with 10% FBS), whereas other studies have used 20% FBS, hypoxic conditions, and a ROCK inhibitor, which enhance the recovery of CFU-Fs (Zhou et al., 2014). Thus, the exact CFU-F efficiencies reported in our study may not be directly comparable to other reports.

Gene-expression microarray of *Grem1*$^+$ versus *Grem1*-negative mesenchymal (CD45$^-$CD31$^-$Ter-119$^-$) cells revealed 1,426 differentially expressed genes (false discovery rate [FDR] < 0.05). The *Grem1*$^+$ population had significantly higher expression of many osteoblast (*Sp7*), chondrocyte (*Acan*), pericytic (*Cpsg4*, *Fap*), and putative stem cell genes (*Klf4*), all of which were confirmed by qPCR (Figures 2G–2M, Table S1E, and Data S1C and S1E). *Grem1*$^+$ cells did not differentially express *Nes* (Figure 2H) or other genes typical of the perisinusoidal mesenchymal niche (Table S1E).

To determine the signaling pathways that were activated in the *Grem1*$^+$ cells, we investigated candidate pathways previously reported to be relevant in MSC differentiation, such as the BMP, TGF-β, FGF/PDGF, and VEGF pathways (Gerber et al., 1999; Ng et al., 2008). Although all of these pathways were statistically significant ($<2.2 \times 10^{16}$ by the $\chi 2$ test), only the genes in the Bmp-activating pathway were consistently increased. *Bmp2*, *Bmp5*, *Bmp6*, the Bmp receptor *Acvr1*, and the BMP signaling target gene *Id2* were all upregulated in *Grem1*$^+$ versus *Grem1*-negative mesenchymal cells (Data S1F and Table S1F). To support the role of BMP signaling in the *Grem1*$^+$ population, we performed qPCR on 23 clones derived from *Grem1*$^+$ bone marrow cells. *Id2* was expressed in 100% of clones, and *Bmp2* was expressed in 91%ofclones. Furthermore, using flow cytometry, pSmad1,5, a marker of BMP signaling, was detected in 37.5% of *Grem1*$^+$ versus 5.8% of *Grem1*-negative freshly sorted cells (Data S1G, p = 0.004). In contrast, genes identified in the TGF-β, FGF/PDGF, and VEGF pathways were found to be both activators and repressors and so did not generate a coherent signal constituting pathway activation (Data S1F, S1H, and S1I).

We also used an unbiased analysis in which all differentially expressed genes in *Grem1*$^+$ versus *Grem1*-negative cells (fdr < 0.05) were evaluated against the KEGG and Reactome

databases. Pathways with a gamma fdr < 0.05 are included in Table S1G (KEGG) and Table S1H (Reactome). The top 3 significant KEGG pathways, the ECM-receptor interaction, PI3K-Akt signaling, and focal adhesion pathways, were all activated according to Pathway Guide's statistical criterion. Differentially expressed genes from these pathways are given in Tables S1I– S1K. Many of the genes upregulated in these pathways are involved in differentiation into bone and cartilage and include the following: chondroadherin, cartilage oligomeric matrix protein, fibroblast growth factors, collagens, integrins, and cyclins. Taken together, BMP signaling along with ECM-receptor interaction, PI3K-Akt signaling, and focal adhesion pathways were all significantly activated in the *Grem1*$^{+}$ cells and are likely to be important either in determining or as a consequence of the *Grem1*$^{+}$ cells' osteochondral lineage potential.

The expression profile of *Grem1*$^{+}$ cells was enriched for genes implicated in bone and cartilage, rather than adipocytic, differentiation (Data S1J; Tables S1L–S1N). Furthermore, *Grem1*$^{+}$ cells, and their derivative clones, expressed active inhibitors of adipogenesis (e.g., *Nr2f2*; Data S1K; Xu et al., 2008). The exact molecular explanation for the more restricted mesenchymal repertoire of *Grem1*$^{+}$ cells, however, remains to be confirmed.

Further qPCR analysis of 23 *Grem1*$^{+}$ cell-derived clones confirmed the mesenchymal homogeneity of *Grem1* cells and their derivative clones (Data S1L). Interestingly, 100% of the *Grem1*$^{+}$ clones expressed both *Nes* and *Grem1*, and *Grem1* transcripts were also detectable within polyclonal *Nes-GFP* cultures. Thus, endogenous *Grem1* and *Nes* expression are not as mutually exclusive as their respective transgenes in vivo. Finally, *GREM1* is also expressed in human MSCs. We examined three distinct human MSC lines derived from normal bone marrow, normal synovium, or inflamed synovium. All lines expressed *GREM1* (Data S1M).

Grem1 Cells Are Endogenous OCR Stem Cells

Grem1-creER^{T}*;R26-LSL-ZsGreen;Acta2-RFP* mice were induced with perinatal tamoxifen (postnatal day [P] 1, Figure 3A). In these mice, all *Grem1*$^{+}$ cells and their subsequent progeny were labeled by green fluorescence, and any cells expressing *Acta2* were marked by red fluorescence. Twenty-four hours after P1 induction, *Grem1*$^{+}$ (green) cells were present within the primitive mesenchyme and the primary spongiosa of the femur. In contrast, the *Acta2*-expressing (red) stromal cells were localized within the bone marrow (Figure 3B). By P5, *Grem1*$^{+}$ cells had differentiated into columns of chondrocytes (Figures 3C and 3D, green) as well as spindle-shaped stromal cells immediately inferior to the developing growth plate (Figures 3C and 3E).

By using *Grem1-creER*^{T}*;R26-LSL-TdTomato;2.3colGFP* mice, one can track *Grem1*$^{+}$ cells and their progeny by red fluorescence, and osteoblasts are marked by green fluorescence. The *2.3colGFP* mouse is a transgenic line in which GFP expression, driven by a short 2.3 kb promoter element from the rat collagen 1a1 gene, has been used to identify committed osteoblasts (Kalajzic et al., 2002). After 6 weeks, the P1-labeled *Grem1*$^{+}$ cells had differentiated into reticular marrow stromal cells (red), chondrocytes (red), and osteoblasts (yellow), all concentrated within the peritrabecular bone area (Figures 3F–3I). Many of the reticular marrow stromal cells anatomically spanned perivascular and endosteal regions and

were CD105$^+$ by immunostaining (Figure S3A). As early as 4 weeks (P28) following P1 induction, *Grem1*$^+$ cells give rise to approximately 64% of the bone and 50% of the chondrocytes within the metaphysis and epiphysis, albeit with little contribution to diaphyseal bone (Figure S3B).

To prove that the fluorescent cells represented clonal populations, we generated *Grem1-creERT;R26-Confetti* mice and again induced at P1. Single-color clones of chondrocytes and marrow stromal cells were present by 6 weeks, confirming single-cell multipotentiality (Figures 3J and 3K). Our Monte Carlo simulation confirmed that the majority (>90%) of patches of adjacent identically colored cells ("clones") were likely to be monoclonal in origin (see Experimental Procedures).

Approximately 12 months after adult (6–8 weeks, Figure 3L) tamoxifen induction of *Grem1-creERT;R26-LSL-TdTomato* mice (and *Grem1-creER^T;R26-LSL-ZsGreen*, mice*)*, we found that *Grem1*$^+$ cells had differentiated into columns of chondrocytes (Figures 3M and 3N), articular cartilage (Figure S3C), reticular marrow stromal cells (Figure 3O), periosteal cells (Figure 3P), diaphyseal osteoblasts (Figure S3D), and osteocytes (Figure 3P). No adipocytes, either in the femurs (Figure S3E) or in the vertebral bodies (Figure S3F), were derived from adult *Grem1*$^+$ cells, even at 1 year after tamoxifen induction. Fluorescently labeled *Grem1*$^+$ cells harvested from the bone marrow after 1 year could still self-renew in vitro. The harvested *Grem1*$^+$ cells in culture formed large colonies, which were clonally expanded (using cloning cylinders) to prove that they retained clonal in vitro multipotentiality, even 12 months after adult tamoxifen induction (Figure S3G). Again, in vitro differentiation was skewed to osteoblast and chondrocyte (Figures S3G–S3J), with little in vitro adipogenesis (Figure S3H). These results indicate that expression of *Grem1* also identified adult multipotent stem cells.

To confirm that *Grem1*$^+$ cells were functional, postnatal skeletal stemcells, we generated *Grem1-creER^T;R26-LSL-ZsGreen;R26-LSL-DTA* mice and *Grem1-creER^T;R26-LSL-ZsGreen* littermate and related controls. In these mice, *Cre*-mediated excision of a STOP signal leads to the expression of the Diphtheria toxin (DTA) and thus ablation of *Grem1*-expressing cells. We administered four daily doses of 2 mg subcutaneous tamoxifen starting at P9 and measured total body and left femoral bone volume by microcomputed tomography (CT) at P23 (Quantum FX Micro-CT, Perkin-Elmer; Figures S4A–S4C). *Grem1* cells were incompletely ablated, although reduced, as assessed by the proportion of *ZsGreen*-expressing cells in the bone marrow (Figure S4A). The DTA$^+$ mice were significantly smaller than the controls (Figure S4B). There was a significant difference infemoral volume between the groups and a trend toward reduced total bone volume in the DTA versus the control mice (Figure S4C). We noted that the major site of *Grem1*-driven recombination at P23, after P9 induction, was within the femoral epiphysis (nearly 60% of the epiphyseal bone was labeled). Therefore, we examined anatomically comparable sections in *Grem1* DTA versus control mice and measured the fraction of mineralized bone in the femoral epiphysis. Here too, the trabecular bone fraction was significantly reduced in DTA mice versus control mice (Figure S4D). This suggested a functional role of *Grem1*$^+$ cells in postnatal skeletogenesis. We acknowledge, however, that ablation of extra-skeletal *Grem1*$^+$ cells may have indirectly contributed, at least in part, to the impaired skeletogenesis.

We measured the expression of *Grem1*, *Nes*, *Runx2*, and *Sox9* by whole-mount in situ hybridization during the earliest stages of hindlimb bud development, i.e., embryonic day (E) 9.5, E10.5, E11.5, and E12.5 (Figure 4A). *Grem1* was expressed at the onset of hindlimb development, E9.5. *Nes* was not expressed within the hindlimb at these stages. To confirm that *Grem1* marked a multipotent mesenchymal stem/progenitor cell during development, we administered tamoxifen to pregnant *Grem1-creERT;R26-LSL-TdTomato* dams at E13.5. Consistent with the in situ hybridization findings, *Grem1* was expressed within much of the primitive hindlimb mesenchyme within the embryos and gave rise to almost all of the cells within the primitive mesenchyme and the primary spongiosa by E21 (Figures S4E and S4F).

Taken together, these results confirm that *Grem1* expression marked a new, endogenous skeletal stem cell, in development and adulthood, which lacked any significant capacity for adipogenesis. As a result, it does not meet the minimal criteria for MSCs (Dominici et al., 2006). Thus, we named these *Grem1*$^+$ stem cells as osteochondroreticular "OCR stem cells" in reference to the earlier concept of the osteochondroprogenitor (Ducy et al., 1997).

Perisinusoidal *Nes-GFP*$^+$ Cells May Not Be Skeletal Stem Cells during Early Life

The previously published *Nes-cre* and *Nes-creER*^{T} lines may not reliably identify the perisinusoidal *Nes-GFP* cells that are purported to be endogenous MSCs (Ding et al., 2012; Méndez-Ferrer et al., 2010). Thus, we used a different transgenic *Nes-creER*^{T} line in an attempt to better understand the lineage potential of *Nes-GFP*$^+$ perisinusoidal MSCs (Dranovsky et al., 2011). Compared to previously reported *Nes* reporter mouse lines, the transgenic *Nes-creER*^{T} line used here had a different *Nes* regulatory sequence directing the expression of *creER*^{T} (Dranovsky et al., 2011). Following P1 tamoxifen induction of *Nes-creER*^{T}*;R26-LSL-TdTomato;Nes-GFP* mice (Figure 4B), *Nes-creER*^{T} recombined *R26-LSL-TdTomato* in approximately 4% of all bone marrow *Nes-GFP* cells by 6–8 weeks (Figure 4C). This included metaphyseal (Figure 4D), periarteriolar (Figure 4E), and perisinusoidal *Nes-GFP* cells (Figures 4F–4H). In keeping with previous perisinusoidal lineage-tracing studies, this *Nes-creER*^{T} line did not generate cartilage or trabecular bone by 6–8 weeks (Ding et al., 2012; Mizoguchi et al., 2014). The only osteochondral cells that were traced consisted of rare, isolated osteocytes embedded within the diaphyseal cortical bone (Figure 4H). Our findings suggest that perisinusoidal cells, labeled by *Nes-GFP*, may not be the principal skeletal stem cells during development or early postnatal life (Ding et al., 2012; Mizoguchi et al., 2014; Zhou et al., 2014). It is quite possible, however, that the endogenous *Nes* geneor other *Nes*-transgenic lines could be expressed in postnatal skeletal stem/progenitor cells, but that these cells were not captured by our lineage-tracing strategy in young (<8-week-old) mice.

Grem1$^+$ OCR Stem Cells Contribute to Fracture Repair

Do adult *Grem1* OCR stem cells respond to skeletal injury? Adult *Grem1*$^+$ cells do not overlap with *2.3colGFP*$^+$ osteoblasts. *Grem1*$^+$ cells are, however, adjacent to osteoblasts in vivo and during early adherent bone marrow stromal culture (Figures 5B and 5C). Surgical fracture with internal fixation of the femur in *Grem1-creER*^{T}*;R26-LSL-TdTomato; 2.3colGFP* mice (performed 1 week after adult induction with tamoxifen) (Figures 5A and 5D) resulted in *Grem1*$^+$ OCR stem cell expansion and differentiation into *2.3colGFP*-

positive (and osteocalcin-positive, Figure S5D) osteoblasts and *2.3colGFP*-negative, Sox9$^+$ chondrocytes within the fracture callus (Figures 5E–5H and S5A–S5C). The *Grem1*$^+$ OCR stem cell lineage, as defined by red fluorescence, contributed approximately 28% of osteoblasts (red and 2.3colGFP green) and 14% of chondrocytes (defined by Sox9 immunostaining and/or by hematoxylin and eosin staining [H&E] on serial sections) within the fracture callus.

Next, we tested whether *Grem1*$^+$ cells could be transplanted into the fracture site. We harvested and expanded a clonal population of *Grem1*$^+$ OCR stem cells. This clone, mixed with hydrogel, was applied to the fracture site at the time of injury and engrafted into the callus of the recipient wild-type mice (Figures 5I and 5J). The transplanted cells differentiated into osteoblasts (alkaline phosphatase-expressing) within the fracture callus (Figure 5K). OCR stem cells self-renewed within the callus and were recovered from the recipient animals and rapidly expanded again in fracture callus cultures (Figure 5L). The *Grem1*$^+$ OCR stem cells cultured from the fracture callus and expanded in vitro could be serially transplanted into a second fracture (Figure S5E). Thus, *Grem1* expression identifies developmental and adult, both physiological and reactive, endogenous OCR stem cells amenable to serial transplantation.

Grem1 Expression also Defines a New iRSC

Could *Grem1* also mark extramedullary connective tissue stem cells? The small intestine was selected as our extramedullary organ of interest because the gut is known to contain multipotent mesenchymal stromal cells (Powell et al., 2011). It is worth emphasizing that we searched for a connective tissue stem cell within the lamina propria and not for an epithelial stem cell, such as that previously identified by *Lgr5* expression (Barker et al., 2007). Furthermore, the small intestine does not contain bone and cartilage, and thus we were not expecting to find a bona fide OCR stem cell. Rather, we were interested in testing for an organ-relevant connective tissue stem cell, sharing *Grem1* expression and the defining stem cell characteristics of self-renewal and multipotentiality. The connective tissue immediately beneath the intestinal epithelium is a mesenchymal sheath that invests the entire intestinal gland (Powell et al., 2011). Adult *Grem1* recombination (24 hr after 6 mg of tamoxifen by oral gavage, *Grem1-creER^T;R26-mT/mG*) identified single cells (*Grem1*$^+$ = green) immediately beneath the epithelium at the junction between the small-intestinal crypt and villus, a region known as the intestinal isthmus (Figures 6A and 6B). In situ hybridization confirmed *Grem1* expression within periepithelial isthmus cells, and these cells were also positive in the *Grem1-LacZ* knockin line (Data S2A–S2F) (Khokha et al., 2003).

Single periepithelial *Grem1* cells divided slowly (BrdU incorporation over 1 month of continuous dosing; Data S2G). Over time, the fluorescently tagged *Grem1*$^+$ cells gave rise to reticular, periepithelial mesenchymal lineages throughout both the crypt and villus sheaths (Figures 6B–6E). The *Grem1*$^+$ cells differentiated into both *Acta2*-positive myofibroblasts (Figure 6F) and *Acta2*-negative, but *Ng2*-positive, stromal cells (Data S2H). *Grem1* cells gave rise to an intricate reticular network of cells that invested the entire gland (Figures 6B–6E, Movie S1). The *Grem1* lineage was distinct from the closely associated s100b (Figure S5I) and *Nes-GFP* positive periepithelial glial sheath (Data S2J) (Belkind-Gerson et al.,

2013). The *Grem1*$^{+}$ cell lineage was intimately related to the overlying intestinal epithelium (Figures 6G and Data S2K). After 6 to 9 months, intestinal *Grem1* cells had expanded to give rise to the mesenchymal sheath subjacent to the *Lgr5*$^{+}$ crypt base columnar stem cell zone (Figures 6B, 6C, and 6E) (Barker et al., 2007). After 12 months, the cells had also renewed the periepithelial mesenchymal sheath to the tip of the villi (Figure 6B). The *Grem1*$^{+}$ cells at the isthmus self-renewed so that their fluorescently tagged lineage persisted across the entire crypt-villus axis for at least 2 years after adult tamoxifen induction (Data S2L). Perinatal induction at P1 led to accelerated intestinal mesenchymal tracing (at 6 weeks), providing further proof of the clonality of the *Grem1* lineage within the mesenchymal sheath (*Grem1-creER*^{T}*;R26-Confetti* mice; Data S2M). The *Grem1* lineage also identified small-intestinal CFU-Fs (Data S2N). Similar patterns of lineage tracing were evident throughout the entire gastrointestinal tract, including the stomach (Data S2O). *Grem1* also identified a progenitor population within the skin (Data S2O). The exact nature of these cells, however, requires further study.

Extending the concept of connective tissue stem cells to extramedullary mesenchyme, however, requires that the model be rigorously validated in vivo. We adapted a protocol for generating tissue-engineered small intestines (TESIs) to test whether *Grem1*$^{+}$ intestinal mesenchymal cells could be transplanted to generate the small-intestinal, periepithelial mesenchymal sheath within the recipient's TESI graft (Levin et al., 2013). *Grem1-creER*^{T}*;R26-LSL-TdTomato* donor small-intestinal organoid units were transplanted into the omentum of recipient wild-type mice. Only one or two *Grem1*$^{+}$ cells were present within the harvested donor units (Figure 6H), but they were able to expand and restore the intestinal mesenchymal sheath in the TESI (Figures 6I and Data S2P). Thus, small-intestinal *Grem1*$^{+}$ cells self-renew and clonally generate multiple distinct, compartment-relevant mesenchymal lineages and can be transplanted to recapitulate the periepithelial mesenchymal sheath, confirming that they are connective tissue stem cells. In this context, we refer to them as iRSCs. We use this term, iRSCs, to reflect their morphology and the reticular network formed by these cells and in reference to their *Grem1*-expressing reticular counterparts in the bone marrow.

Discussion

Despite intensive investigation, the identity of an endogenous “skeletal stem cell” has remained elusive. We generated an inducible *Cre* line, driven by the enhancer elements of the BMP antagonist *Grem1*, to identify and lineage trace rare skeletal stem cells in vivo. Adult *Grem1* OCR stem cells were found beside the growth plate and the trabecular bone, where they generated and maintained articular and growth plate cartilage, bone and reticular marrow stromal cells, but not fat. Adult *Grem1* OCR stem cells did not overlap with perisinusoidal *Nes-GFP* MSCs, appear to be more clonogenic in vitro than *Nes-GFP* MSCs, and make a far greater contribution to early postnatal skeletogenesis than traditional perisinusoidal MSCs (Ding et al., 2012; Zhou et al., 2014). This study complements the existing, perisinusoidal MSC model of postnatal skeletogenesis (Figure 7) (Bianco et al., 2013). We have also identified *Grem1*-expressing, reticular stem cells in the small intestine, the iRSCs, that self-renew to maintain the multilineage periepithelial, mesenchymal sheath. The iRSCs are distinct from, but analogous to, their *Grem1*-expressing OCR stem cells in

the bone. Each has an organ-appropriate mesenchymal repertoire, but these *Grem1*-expressing stem cells are united by their capacity for self-renewal, multipotentiality, and continued functionality following transplantation.

Bone and cartilage could develop from a population of dedicated and committed postnatal progenitors (as with pancreatic beta cells). Alternatively, they could arise from a multipotent stem cell capable of generating bone, cartilage, and accessory elements, such as adipocytes and pericytes. A third model, which we favor, suggests that discrete stem cells make temporal and lineage-specific contributions to skeletal development and maintenance (Takashima et al., 2007). That is, the OCR stem cell is a substantial skeletal stem cell in development and early postnatal life, but over time, the perisinusoidal MSC increases its contribution to skeletal homeostasis, such that ultimately adult mesenchymal tissues are maintained from two separate, but complementary, stem cell pools (Figure 7).

Perisinusoidal *Nes-GFP* MSCs fulfill the in vitro criteria of MSCs (Méndez-Ferrer et al., 2010); however, they make little endogenous contribution to skeletogenesis, at least during early life (Figure 4) (Ding et al., 2012; Mizoguchi et al., 2014; Zhou et al., 2014). In contrast, OCR stem cells are most active during development, giving rise to trabecular bone, cartilage, and reticular marrow stromal cells. Although it was reported that all adult bone marrow CFU-Fs are *Nes-GFP*$^+$ (Méndez-Ferrer et al., 2010), *Grem1* OCR stem cells are negative for *Nes-GFP* and yet are clonogenic (Figures 1D–1G). We believe that this discrepancy may arise from differences in our isolation and culture of the bone marrow. Bone marrow *Nes-GFP* cells were originally isolated by bone flush without reported collagenase digestion (Méndez-Ferrer et al., 2010), which enhances the yield of CFU-Fs (Morikawa et al., 2009). Enzymatic digestion was essential for liberating *Grem1*$^+$ cells from the bone and bone marrow. There were also differences in our mesenchymal sorting strategy. We classified CD45$^-$CD31$^-$Ter-119$^-$ triple-negative cells as bone marrow mesenchyme, as previously reported (Park et al., 2012), whereas in the original *Nes-GFP* MSC study, CD45$^-$ alone was used as the mesenchymal arbiter (Méndez-Ferrer et al., 2010). This may have resulted in some CD31$^+$ endothelial cells being collected, and given that *Nes-GFP* is expressed in bone marrow endothelium (Ono et al., 2014), it is conceivable that the mesenchymal *Nes-GFP* population we evaluated (CD45$^-$CD31$^-$Ter-119$^-$*Nes-GFP*$^+$) was different from that evaluated previously (Méndez-Ferrer et al., 2010).

Developmentally, *Nes-GFP*$^+$ and *Lepr-cre*$^+$ perisinusoidal MSCs and *Grem1*$^+$ OCR stem cells could represent different cells within a common lineage. Although this remains a possibility, we note that *Grem1*$^+$ cells do not give rise to *Nes-GFP* cells, even 10 months after tamoxifen induction. Similarly, P1 induction of *Nes-creER*^{T}, or constitutive lineage tracing of *Lepr*$^+$ cells using the *Lepr-cre* (Zhou et al., 2014), did not lead to significant genetic recombination of trabecular bone or cartilage in early life. In contrast, trabecular bone and cartilage are clearly derived from *Grem1*$^+$ cells. Thus, based on our data, and those of others (Ding et al., 2012; Mizoguchi et al., 2014; Zhou et al., 2014), we conclude that there are at least two skeletogenic stem cells contributing to postnatal bone (Figure 7). Remarkably, only OCR stem cells appear to generate articular and growth-plate cartilage during development, and the contribution of perisinusoidal MSCs is modest until later adulthood, at which point the perisinusoidal MSCs are ultimately capable of generating fat,

bone, and cartilage, particularly following injury (Figure 7) (Zhou et al., 2014). We propose that the OCR stem cell is vital in skeletogenesis, whereas the traditional perisinusoidal MSCs gradually increase their skeletal contribution over time. Traditional MSCs appear to partner with OCR stem cells to repair bone in the event of fracture, but this may again depend on the developmental stage at which the injury occurs (Figure 7).

In contrast to perisinusoidal MSCs, the *Grem1* OCR stem cells did not generate adipocytes in vivo or in vitro. Thus, although the *Grem1*$^+$ cell is multipotent (giving rise to osteoblasts, chondrocytes, and reticular marrow stromal cells) and a bone fide stem cell, it is not the usual origin of adipocytes, at least under the conditions examined. The relative ascendency of perisinusoidal MSCs in later adulthood could potentially explain the increasing adipogenesis evident in the bone marrow in later life.

Our selected marker, *Grem1,* is a BMP antagonist that is especially important for skeletal patterning and contributes to postnatal skeletal homeostasis (Bénazet et al., 2009; Canalis et al., 2012; Khokha et al., 2003). BMP signaling in skeletogenesis expands primitive mesenchymal cells, laying the foundation for subsequent endochondral ossification (Kronenberg, 2003). Despite expression of the BMP antagonist *Grem1*, BMP signaling was elevated in OCR stem cells compared to the *Grem1*-negative mesenchymal cells. Increased BMP signaling is consistent with the location of OCR stem cells, which is immediately adjacent to the BMP-producing growth plate, and our microarray and qPCR data suggest that OCR stem cells also produce Bmps that may act in an autocrine fashion (Kronenberg, 2003).

Researchers have harvested MSC-like cells from many different adult organs (Crisan et al., 2008). In the small intestine, single *Grem1*$^+$ iRSCs immediately subjacent to the epithelium at the junction between the small-intestinal crypt and villus (the intestinal isthmus) undergo slow division, to ultimately generate the entire periepithelial sheath of the crypt and villus, forming a closely connected mesenchymal network. In adulthood, this process takes about one year, during which time the *Grem1* iRSCs give rise to both *Acta2*-positive myofibroblasts and *Acta2*-negative periepithelial fibroblasts, thus establishing their endogenous self-renewal and compartment-specific multipotentiality.

The *Grem1*$^+$ iRSC is adifferent cell from the *Grem1*$^+$ OCR stem cell, with discrete functions and distinct lineage potential, namely periepithelial mesenchyme rather than bone and cartilage. Nevertheless, it shares with the *Grem1* OCR stem cell a stellate morphology, relative quiescence, and most importantly the properties of endogenous self-renewal and mesenchymal multipotentiality.

The stem cell responsible for developing bone and cartilage in vivo, the OCR stem cell, appears to show great promise for skeletal tissue engineering, particularly for conditions such as osteoarthritis, osteoporosis, and fracture. *Grem1* OCR stem cells could be harvested from a donor animal, expanded in vitro, and transplanted, both directly and serially, into the femurs of fractured recipient animals, resulting in osteochondral differentiation in the callus. Future studies will be needed to compare the ability of *Grem1*$^+$ cells to heal skeletal diseases relative to those of other mesenchymal progenitor populations. Our discovery of analogous

iRSCs is also likely to be important in intestinal replacement and repair and may inform mesenchymal hierarchy in other complicated connective tissues, including the tumor microenvironment.

Taken together, our findings confirm the existence and relevance of bone, cartilage, and reticular stromal stem cells and present a paradigm shift in understanding the diverse origins of connective tissues in health, aging, and disease.

Experimental Procedures

Mice

We used the following lines: *Nes-GFP* (Mignone et al., 2004), *Nes-CreER^{T2}* (Dranovsky et al., 2011), Grem1-LacZ (Khokha et al., 2003), Acta2-RFP (Magness et al., 2004), R26-LSL-ZsGreen (Madisen et al., 2010), R26-LSL-TdTomato (Madisen et al., 2010), R26-LSL-mT/mG (Muzumdar et al., 2007), *2.3Col*GFP (Kalajzic et al., 2002), R26-LSL-Confetti (Snippert et al., 2010), and R26-LSL-DTA (Voehringer et al., 2008) (Table S1B). The R26-LSL-mT/mG was used in the intestine to better appreciate intestinal architecture, but for the bone marrow, either the R26-LSL-ZsGreen or the R26-LSL-TdTomato was used to enable the addition of a second reporter, such as *Nes-GFP, 2.3colGFP* or *Acta2-RFP*. We generated the *Grem1-CreER^{T}* transgenic by BAC recombineering (clone RP24-317C19), as previously described (Sharan et al., 2009). The recombineering primers amplified the CreER^{T}-pA-fNf cassette with 60 bp homology arms upstream and downstream of the Grem1 translational start site in exon 2 (Table S1A). We generated three founder lines. Line 3 displayed the greatest recombination following adult tamoxifen induction, and it was backcrossed six generations to C57BL/6J. All experiments were performed according to the guidelines of the Institute of Comparative Medicine at Columbia University.

Marrow Stromal Cell Isolation

Long bones of the arms and legs were harvested and gently disrupted using a mortar and pestle, in PBS with 2% FBS and 1 mM EDTA. The bone and all of the liberated bone marrow were collected and digested in 0.25% collagenase type I (Worthington, Lakewood, NJ, USA, LS004196) in PBS with 20% FBS, for cell culture or flow cytometry.

Clonal In Vitro Bone Marrow MSC Culture, Clonogenicity Assays, and Differentiation

Marrow stromal cells were plated at clonal density and cultured for 14 days in αMEM + 10% defined MSC FBS + 1% penicillin/streptomycin. The total number of colonies, defined as ≥50 cells, were stained with Giemsa. The number of clones were reported as (CFU-Fs)/1,000 cells plated. For differentiation, single recombined clones were isolated using cloning cylinders and then expanded and split for differentiation using Invitrogen StemPro differentiation products into adipocytes, chondrocytes, and osteoblasts. All in vitro differentiation reported in this study is clonal.

Fracture Studies

Adult *Grem1-creER^{T};R26-LSL-TdTomato;2.3ColGFP* mice were induced with tamoxifen with a 1 week washout period before fracture. Unilateral femoral osteotomy was internally

fixed by an angiocatheter. Femurs were harvested at 7 days. For the fracture transplantation, a single *Grem1*-derived clone (after adult in vivo induction) was expanded in vitro and then 500×10^6 cells were mixed with a HyStem-C(TM) Hydrogel Kit (Glycosan) and injected around the fracture sites of the recipient wild-type mice. The fractured bones were harvested at 7days. Some of the fracture callus was recultured to recover the donor $Grem1^+$ cells. The fractures were imaged by X-ray and a Kodak In Vivo Multispectral Imaging System FX (carestream Health) specific for TdTomato fluorescence.

Tissue-Engineered Small Intestines

Organoid units were harvested from 3-week-old, P1 tamoxifen-induced *Grem1-creERT;R26-LSL-TdTomato* donor mice and transplanted into 8 wild-type adult C57BL/6 mice. The procedure was otherwise performed as previously described (Levin et al., 2013) with the TESIs harvested at 4 weeks post-implantation for analysis.

Supplementary Material

Refer to Web version on PubMed Central for supplementary material.

Authors

Daniel L. Worthley[1,2,3,4], Michael Churchill[1], Jocelyn T. Compton[5], Yagnesh Tailor[1], Meenakshi Rao[6], Yiling Si[1], Daniel Levin[7], Matthew G. Schwartz[8], Aysu Uygur[8], Yoku Hayakawa[1], Stefanie Gross[9], Bernhard W. Renz[1], Wanda Setlik[10], Ashley N. Martinez[5], Xiaowei Chen[1], Saqib Nizami[5], Heon Goo Lee[5], H. Paco Kang[5], Jon-Michael Caldwell[5], Samuel Asfaha[1], C. Benedikt Westphalen[1,11], Trevor Graham[12], Guangchun Jin[1], Karan Nagar[1], Hongshan Wang[1], Mazen A. Kheirbek[13], Alka Kolhe[1], Jared Carpenter[1], Mark Glaire[1], Abhinav Nair[1], Simon Renders[1], Nicholas Manieri[14], Sureshkumar Muthupalani[15], James G. Fox[15], Maximilian Reichert[16], Andrew S. Giraud[4], Robert F. Schwabe[1], Jean-Phillipe Pradere[1,17], Katherine Walton[18], Ajay Prakash[18], Deborah Gumucio[18], Anil K. Rustgi[16], Thaddeus S. Stappenbeck[14], Richard A. Friedman[19], Michael D. Gershon[10], Peter Sims[20], Tracy Grikscheit[7], Francis Y. Lee[5], Gerard Karsenty[9], Siddhartha Mukherjee[1,21,*], and Timothy C. Wang[1,21,*]

Affiliations

[1]Department of Medicine and Irving Cancer Research Center, Columbia University, New York, NY 10032, USA

[2]Department of Medicine, University of Adelaide, SA, 5005, Australia

[3]Cancer theme, South Australian Health and Medical Research Institute, SA, 5001, Australia

[4]Murdoch Children's Research Institute, Royal Children's Hospital, Vic., 3052, Australia

[5]Department of Orthopedic Surgery, Columbia University Medical Center, New York, NY 10032, USA

[6]Department of Pediatrics, Columbia University, New York, NY 10032, USA

[7]Children's Hospital Los Angeles, Saban Research Institute, Keck School of Medicine of the University of Southern California, Los Angeles, CA 90027, USA

[8]Department of Genetics, Harvard Medical School, Boston, MA 02114, USA

[9]Department of Genetics and Development, Columbia University, New York, NY 10032, USA

[10]Department of Pathology and Cell Biology, Columbia University, New York, NY 10032, USA

[11]Department of Internal Medicine III, University Hospital Munich, Ludwig-Maximilians-University Munich - Campus Groβhadern, Munich 81377, Germany

[12]Barts Cancer Institute, Barts and the London School of Medicine and Dentistry, Queen Mary University of London, London EC1M 6BQ, UK

[13]Department of Psychiatry, Columbia University, New York, NY 10032, USA

[14]Department of Pathology and Immunology, Washington University, St. Louis, MO 63110, USA

[15]Division of Comparative Medicine, Massachusetts Institute of Technology, Cambridge, MA 02139, USA

[16]Division of Gastroenterology, Departments of Medicine and Genetics, Abramson Cancer Center, University of Pennsylvania Perelman School of Medicine, Philadelphia, PA 19104, USA

[17]Institut National de la Santéet de la Recherche Médicale (INSERM), Université Paul Sabatier, Institut des Maladies Métaboliques et Cardiovasculaires (I2MC)-UMR1048, Toulouse 31432, France

[18]Department of Cell and Developmental Biology, University of Michigan, Ann Arbor, MI 48109, USA

[19]Herbert Irving Comprehensive Cancer Center Biomedical Informatics Shared Resource and Department of Biomedical Informatics, Columbia University, New York, NY 10032, USA

[20]Department of Systems Biology, Columbia University, NY, 10032, USA

Acknowledgments

Thank you to Dr. Liza Phillips. Thank you to all members of the Wang laboratory at Columbia University. Thank you to Professor David Callen, Dr. Miao Yang, and Dr. Laura Vrbanac at the University of Adelaide. Thank you to Dr. Lei Ding for his advice and assistance. Thank you to Dr. Grigori Enikolopov (Cold Spring Harbor Laboratory) and Dr. Rene Hen (Columbia University) for sharing their transgenic mice. Thank you to Dr. Victor Lin for his transgenic advice and to Dr. Brian Eyden for his advice regarding intestinal mesenchymal cells. We are grateful for the following funding: from the NIH to T.C.W. (NIH 5U54 CA126513), to S.M. (R01 RHL115145A), to F.Y.L. from the Robert Carroll and Jane Chace Carroll Laboratories and also the NIH (NIH AR056246 and EB006834), to A.K.R. from the American Cancer Society, and to D.L.W. from the NH&MRC and Menzies Foundation, Cancer Council SA's Beat Cancer Project on behalf of its donors and the State Government of South Australia through the Department of Health, Gastroenterological Society of Australia, the American Gastroenterological Association, the

American Association for Cancer Research, the Royal Australasian College of Physicians, and the Ines Mandl Postdoctoral research fellowship Columbia University.

References

Barker N, van Es JH, Kuipers J, Kujala P, van den Born M, Cozijnsen M, Haegebarth A, Korving J, Begthel H, Peters PJ, Clevers H. Identification of stem cells in small intestine and colon by marker gene Lgr5. Nature. 2007; 449:1003–1007. [PubMed: 17934449]

Belkind-Gerson J, Carreon-Rodriguez A, Benedict LA, Steiger C, Pieretti A, Nagy N, Dietrich J, Goldstein AM. Nestin-expressing cells in the gut give rise to enteric neurons and glial cells. Neurogastroenterol Motil. 2013; 25:61.e7. [PubMed: 22998406]

Bénazet JD, Bischofberger M, Tiecke E, Gonçalves A, Martin JF, Zuniga A, Naef F, Zeller R. A self-regulatory system of interlinked signaling feedback loops controls mouse limb patterning. Science. 2009; 323:1050–1053. [PubMed: 19229034]

Bianco P, Cao X, Frenette PS, Mao JJ, Robey PG, Simmons PJ, Wang CY. The meaning, the sense and the significance: translating the science of mesenchymal stem cells into medicine. Nat Med. 2013; 19:35–42. [PubMed: 23296015]

Canalis E, Parker K, Zanotti S. Gremlin1 is required for skeletal development and postnatal skeletal homeostasis. J Cell Physiol. 2012; 227:269–277. [PubMed: 21412775]

Crisan M, Yap S, Casteilla L, Chen CW, Corselli M, Park TS, Andriolo G, Sun B, Zheng B, Zhang L, et al. A perivascular origin for mesenchymal stem cells in multiple human organs. Cell Stem Cell. 2008; 3:301–313. [PubMed: 18786417]

Delorme B, Ringe J, Pontikoglou C, Gaillard J, Langonné A, Sensebé L, Noël D, Jorgensen C, Häupl T, Charbord P. Specific lineage-priming of bone marrow mesenchymal stem cells provides the molecular framework for their plasticity. Stem Cells. 2009; 27:1142–1151. [PubMed: 19418444]

Ding L, Saunders TL, Enikolopov G, Morrison SJ. Endothelial and perivascular cells maintain haematopoietic stem cells. Nature. 2012; 481:457–462. [PubMed: 22281595]

Dominici M, Le Blanc K, Mueller I, Slaper-Cortenbach I, Marini F, Krause D, Deans R, Keating A, Prockop Dj, Horwitz E. Minimal criteria for defining multipotent mesenchymal stromal cells. The International Society for Cellular Therapy position statement. Cytotherapy. 2006; 8:315–317. [PubMed: 16923606]

Dranovsky A, Picchini AM, Moadel T, Sisti AC, Yamada A, Kimura S, Leonardo ED, Hen R. Experience dictates stem cell fate in the adult hippocampus. Neuron. 2011; 70:908–923. [PubMed: 21658584]

Ducy P, Zhang R, Geoffroy V, Ridall AL, Karsenty G. Osf2/Cbfa1: a transcriptional activator of osteoblast differentiation. Cell. 1997; 89:747–754. [PubMed: 9182762]

Gerber HP, Vu TH, Ryan AM, Kowalski J, Werb Z, Ferrara N. VEGF couples hypertrophic cartilage remodeling, ossification and angiogenesis during endochondral bone formation. Nat Med. 1999; 5:623–628. [PubMed: 10371499]

Grcevic D, Pejda S, Matthews BG, Repic D, Wang L, Li H, Kronenberg MS, Jiang X, Maye P, Adams DJ, et al. In vivo fate mapping identifies mesenchymal progenitor cells. Stem Cells. 2012; 30:187–196. [PubMed: 22083974]

Hsu DR, Economides AN, Wang X, Eimon PM, Harland RM. The Xenopus dorsalizing factor Gremlin identifies a novel family of secreted proteins that antagonize BMP activities. Mol Cell. 1998; 1:673–683. [PubMed: 9660951]

Jaeger E, Leedham S, Lewis A, Segditsas S, Becker M, Cuadrado PR, Davis H, Kaur K, Heinimann K, Howarth K, et al. Hereditary mixed polyposis syndrome is caused by a 40-kb upstream duplication that leads to increased and ectopic expression of the BMP antagonist GREM1. Nat Genet. 2012; 44:699–703. [PubMed: 22561515]

Kalajzic I, Kalajzic Z, Kaliterna M, Gronowicz G, Clark SH, Lichtler AC, Rowe D. Use of type I collagen green fluorescent protein transgenes to identify subpopulations of cells at different stages of the osteoblast lineage. J Bone Miner Res. 2002; 17:15–25. [PubMed: 11771662]

Khokha MK, Hsu D, Brunet LJ, Dionne MS, Harland RM. Gremlin isthe BMP antagonist required for maintenance of Shh and Fgf signals during limb patterning. Nat Genet. 2003; 34:303–307. [PubMed: 12808456]

Kosinski C, Li VSW, Chan ASY, Zhang J, Ho C, Tsui WY, Chan TL, Mifflin RC, Powell DW, Yuen ST, et al. Gene expression patterns of human colon tops and basal crypts and BMP antagonists as intestinal stem cell niche factors. Proc Natl Acad Sci USA. 2007; 104:15418–15423. [PubMed: 17881565]

Kronenberg HM. Developmental regulation of the growth plate. Nature. 2003; 423:332–336. [PubMed: 12748651]

Levin DE, Sala FG, Barthel ER, Speer AL, Hou X, Torashima Y, Grikscheit TC. A “living bioreactor” for the production of tissue-engineered small intestine. Methods Mol Biol. 2013; 1001:299–309. [PubMed: 23494439]

Madisen L, Zwingman TA, Sunkin SM, Oh SW, Zariwala HA, Gu H, Ng LL, Palmiter RD, Hawrylycz MJ, Jones AR, et al. A robust and high-throughput Cre reporting and characterization system for the whole mouse brain. Nat Neurosci. 2010; 13:133–140. [PubMed: 20023653]

Magness ST, Bataller R, Yang L, Brenner DA. A dual reporter gene transgenic mouse demonstrates heterogeneity in hepatic fibrogenic cell populations. Hepatology. 2004; 40:1151–1159. [PubMed: 15389867]

Méndez-Ferrer S, Michurina TV, Ferraro F, Mazloom AR, Macarthur BD, Lira SA, Scadden DT, Ma'ayan A, Enikolopov GN, Frenette PS. Mesenchymal and haematopoietic stem cells form a unique bone marrow niche. Nature. 2010; 466:829–834. [PubMed: 20703299]

Michos O, Panman L, Vintersten K, Beier K, Zeller R, Zuniga A. Gremlin-mediated BMP antagonism induces the epithelial-mesenchymal feedback signaling controlling metanephric kidney and limb organogenesis. Development. 2004; 131:3401–3410. [PubMed: 15201225]

Mignone JLJ, Kukekov VV, Chiang ASA, Steindler DD, Enikolopov GG. Neural stem and progenitor cells in nestin-GFP transgenic mice. J Comp Neurol. 2004; 469:311–324. [PubMed: 14730584]

Mitola S, Ravelli C, Moroni E, Salvi V, Leali D, Ballmer-Hofer K, Zammataro L, Presta M. Gremlin is a novel agonist of the major proangiogenic receptor VEGFR2. Blood. 2010; 116:3677–3680. [PubMed: 20660291]

Mizoguchi T, Pinho S, Ahmed J, Kunisaki Y, Hanoun M, Mendelson A, Ono N, Kronenberg HM, Frenette PS. Osterix marks distinct waves of primitive and definitive stromal progenitors during bone marrow development. Dev Cell. 2014; 29:340–349. [PubMed: 24823377]

Morikawa S, Mabuchi Y, Kubota Y, Nagai Y, Niibe K, Hiratsu E, Suzuki S, Miyauchi-Hara C, Nagoshi N, Sunabori T, et al. Prospective identification, isolation, and systemic transplantation of multipotent mesenchymal stem cells in murine bone marrow. J Exp Med. 2009; 206:2483–2496. [PubMed: 19841085]

Muzumdar MD, Tasic B, Miyamichi K, Li L, Luo L. A global double-fluorescent Cre reporter mouse. Genesis. 2007; 45:593–605. [PubMed: 17868096]

Ng F, Boucher S, Koh S, Sastry KS, Chase L, Lakshmipathy U, Choong C, Yang Z, Vemuri MC, Rao MS, Tanavde V. PDGF, TGF-beta, and FGF signaling is important for differentiation and growth of mesenchymal stem cells (MSCs): transcriptional profiling can identify markers and signaling pathways important in differentiation of MSCs into adipogenic, chondrogenic, and osteogenic lineages. Blood. 2008; 112:295–307. [PubMed: 18332228]

Ono N, Ono W, Mizoguchi T, Nagasawa T, Frenette PS, Kronen-berg HM. Vasculature-associated cells expressing nestin in developing bones encompass early cells in the osteoblast and endothelial lineage. Dev Cell. 2014; 29:330–339. [PubMed: 24823376]

Park D, Spencer JA, Koh BI, Kobayashi T, Fujisaki J, Clemens TL, Lin CP, Kronenberg HM, Scadden DT. Endogenous bone marrow MSCs are dynamic, fate-restricted participants in bone maintenance and regeneration. Cell Stem Cell. 2012; 10:259–272. [PubMed: 22385654]

Powell DW, Pinchuk IV, Saada JI, Chen X, Mifflin RC. Mesenchymal cells of the intestinal lamina propria. Annu Rev Physiol. 2011; 73:213–237. [PubMed: 21054163]

Quante M, Tu SP, Tomita H, Gonda T, Wang SSW, Takashi S, Baik GH, Shibata W, Diprete B, Betz KS, et al. Bone marrow-derived myofibroblasts contribute to the mesenchymal stem cell niche and promote tumor growth. Cancer Cell. 2011; 19:257–272. [PubMed: 21316604]

Sacchetti B, Funari A, Michienzi S, Di Cesare S, Piersanti S, Saggio I, Tagliafico E, Ferrari S, Robey PG, Riminucci M, Bianco P. Self-renewing osteoprogenitors in bone marrow sinusoids can organize a hematopoietic microenvironment. Cell. 2007; 131:324–336. [PubMed: 17956733]

Sharan SK, Thomason LC, Kuznetsov SG, Court DL. Recombineering: a homologous recombination-based method of genetic engineering. Nat Protoc. 2009; 4:206–223. [PubMed: 19180090]

Sneddon JB, Zhen HH, Montgomery K, van de Rijn M, Tward AD, West R, Gladstone H, Chang HY, Morganroth GS, Oro AE, Brown PO. Bone morphogenetic protein antagonist gremlin 1 is widely expressed by cancer-associated stromal cells and can promote tumor cell proliferation. Proc Natl Acad Sci USA. 2006; 103:14842–14847. [PubMed: 17003113]

Snippert HJ, van der Flier LG, Sato T, van Es JH, van den Born M, Kroon-Veenboer C, Barker N, Klein AM, van Rheenen J, Simons BD, Clevers H. Intestinal crypt homeostasis results from neutral competition between symmetrically dividing Lgr5 stem cells. Cell. 2010; 143:134–144. [PubMed: 20887898]

Takashima Y, Era T, Nakao K, Kondo S, Kasuga M, Smith AG, Nishikawa S. Neuroepithelial cells supply an initial transient wave of MSC differentiation. Cell. 2007; 129:1377–1388. [PubMed: 17604725]

Voehringer D, Liang HE, Locksley RM. Homeostasis and effector function of lymphopenia-induced “memory-like” T cells in constitutively T cell-depleted mice. J Immunol. 2008; 180:4742–4753. [PubMed: 18354198]

Zhou BO, Yue R, Murphy MM, Peyer JG, Morrison SJ. Leptin-receptor-expressing mesenchymal stromal cells represent the main source of bone formed by adult bone marrow. Cell Stem Cell. 2014; 15:154–168. [PubMed: 24953181]

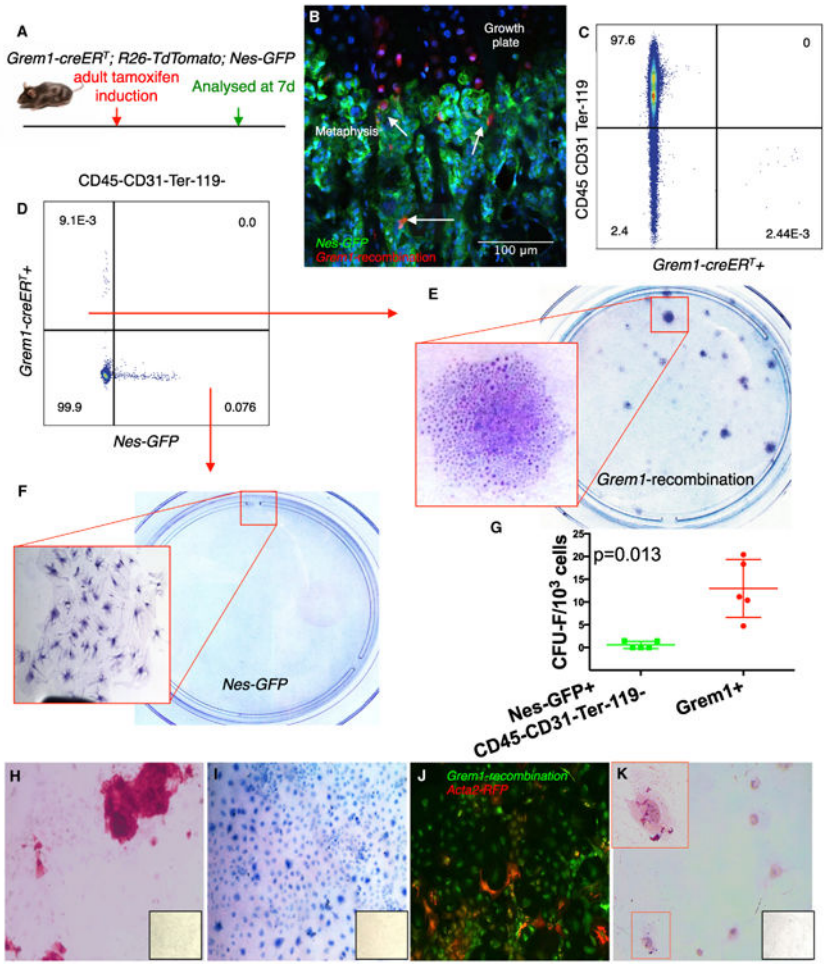

Figure 1. *Grem1* Identifies Rare Adult Multipotent Mesenchymal Stromal Cells

(A) Protocol and (B) *Grem1-creER^T;R26-LSL-TdTomato;Nes-GFP* mouse femur, showing that metaphyseal *Nes-GFP*$^+$ (green) and *Grem1*$^+$ cells (red, white arrows) are distinct.

(C) Adult *Grem1-creER^T;R26-LSL-TdTomato* bone marrow cells are rare and mesenchymal (CD45$^-$CD31$^-$Ter-119$^-$).

(D–G) Adult *Grem1-creER^T;R26-LSL-TdTomato;Nes-GFP* mice: *Grem1* and mesenchymal *Nes-GFP* cells do not overlap, and clonogenicity is greater in the *Grem1*$^+$ versus the mesenchymal *Nes-GFP*$^+$ cells (CD45$^-$CD31$^-$Ter-119$^-$). (E and F) 10 cm cell culture dish; (G) n = 5, data shown with mean ± SD, p = 0.013.

(H–K) *Grem1*$^+$ cells from *Grem1-creER^T;R26-LSL-ZsGreen;Acta2-RFP* mice could be clonally expanded in vitro and differentiated into bone (H) (alizarin red), cartilage (I) (toluidine blue), and myofibroblasts (J) (*Grem1*$^+$ green-derived cells with coexpression of *Acta2* [red]), but very limited adipogenesis (oil red) (K). Lower right insets show equivalent stain in a control marrow culture.

In all graphs, the data are shown with the mean ± SD.

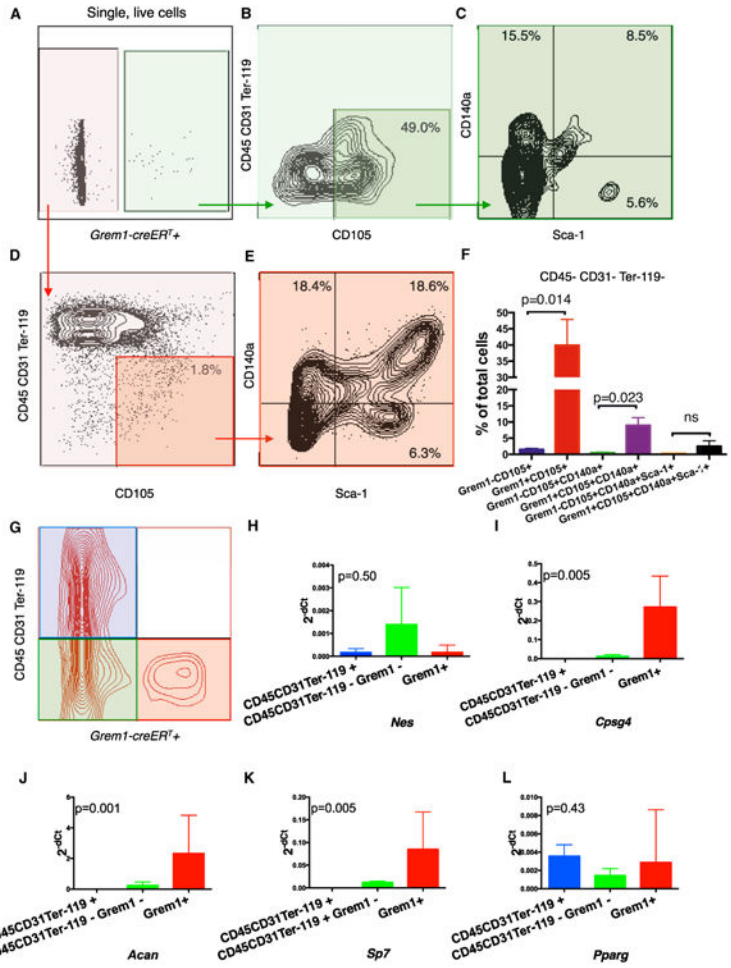

Figure 2. *Grem1*$^+$ Cells Are Enriched for CD105 Bone Marrow Cells with Upregulated Osteochondral versus Adipogenic Gene Expression

(A–F) n = 3, *Grem1*$^+$ cells from adult, collagenase-digested whole bone and bone marrow were compared to the *Grem1*-negative population. On average, 40% (95% CI 20%–60%) of all *Grem1* cells were CD45$^-$CD31$^-$Ter-119$^-$CD105$^+$ compared to only 1.8% of *Grem1*-negative cells (F, p = 0.014). (C) *Grem1*$^+$ cells, however, were not further enriched for other MSC markers CD140a and Sca-1. *Grem1*$^+$ and *Grem1*-negative cells were compared across the increasingly specific immunophenotypes; data shown with mean ± SD.

(G) Microarray was performed to compare the *Grem1*$^+$ (red) to the nonrecombined stromal (CD45$^-$CD31$^-$Ter-119$^-$) population (green); in qPCR, we also sorted and evaluated the CD45CD31Ter-119$^+$ population (blue) that did not contain any recombined cells.

(H) *Grem1*$^+$ cells were not enriched for *Nes* expression.

(I–L) qPCR confirmation of microarray revealed that *Grem1*$^+$ cells had increased expressionof pericytic (*Cpsg4*;I) and osteochondral genes (*Acan* and *Sp7;* J and K) but no association with the adipogenic differentiation gene *Pparg* (L).

In all graphs, the data are shown with the mean ± SD.

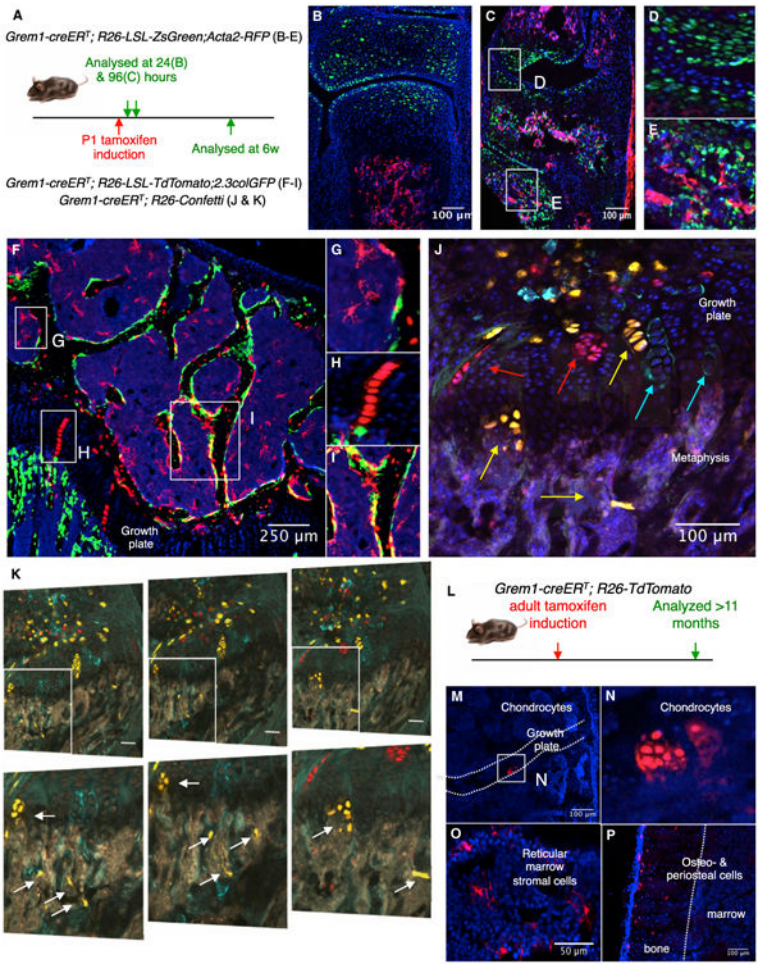

Figure 3. Endogenous *Grem1* Cells Self-Renew and Lineage Trace Bone, Cartilage, and Stroma

(A) Protocol.

(B–E) P1 induction in *Grem1-creER^T;R26-LSL-ZsGreen;Acta2-RFP* mice. (B) At 24 hr after tamoxifen, *Grem1* recombined (green) only within the primary spongiosa of long bones distinct from the *Acta2-RFP* (red) cells in the marrow. But, over the following 96 hr (C), the *Grem1* cells began organizing into chondrocytic columns (D) and differentiated into stromal cells that invade the bone marrow (E) intertwined with *Acta2*-positive (red) cells.

(F–I) *Grem1-creER^T;R26-LSL-TdTomato;2.3colGFP* mice induced at P1, examined at 6 weeks, show that the *Grem1$^+$* cells generate reticular marrow stromal cells (G), chondrocytes in the epiphyseal plate (H), osteoblasts (*2.3colGFP$^+$*, thus yellow) in the trabecular bone (I).

(J) *Grem1-creER^T;R26-Confetti* P1 induction, examined at 6 weeks, revealed clonal populations of chondrocytes, and (K) serial sections confirm mixed clones, yellow clone shown, of chondrocytes and marrow stromal cells, low- and higher-power (inset) images.

(L–P) Adult induction in *Grem1-creER^T;R26-LSL-TdTomato* analyzed 11 months after adult induction (L). *Grem1$^+$* cells had generated chondrocytes (M and N), reticular marrow stromal cells (O), and bone and periosteal cells (red) (P).

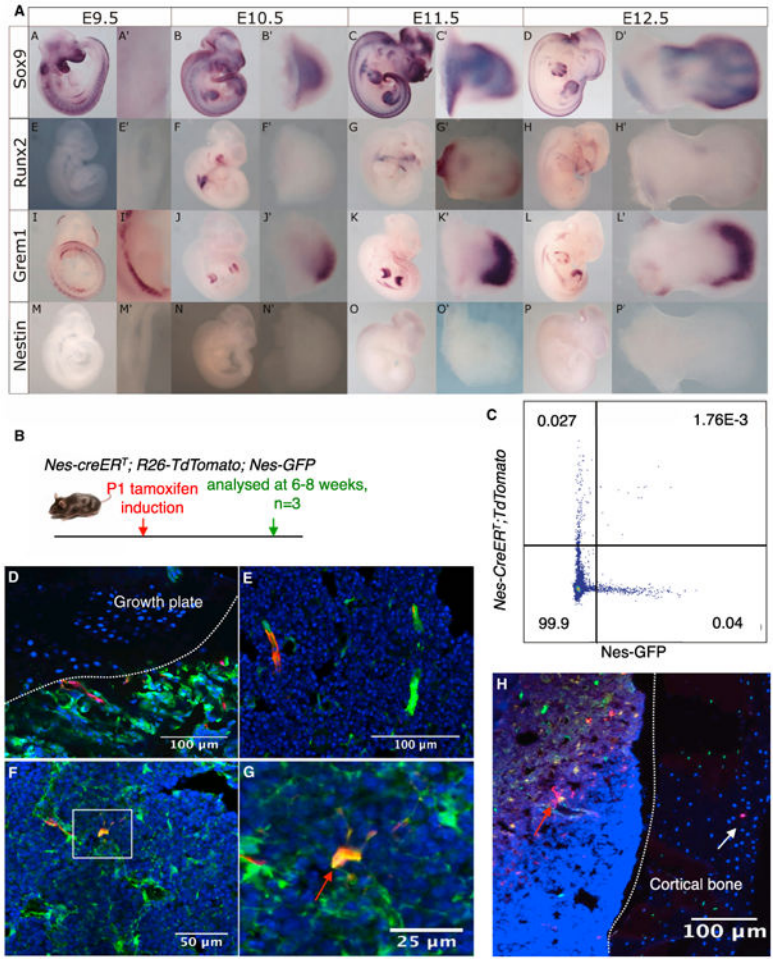

Figure 4. ***Nes-GFP*** **Cells Make Little Contribution to Skeletal Tissues during Early Life**

(A) Whole-mount in situ hybridization on mouse embryos at E9.5, E10.5, E11.5 and E12.5. These embryos were evaluated for *Sox9, Runx2, Grem1*, and *Nes* expression. *Nes-creER^T; R26-LSL-TdTomato; Nes-GFP* mice (n = 3) were generated to lineage trace from *Nes-GFP*-positive cells throughout the bone marrow. These mice were induced at P1 and examined 6–8 weeks after.

(B) Protocol.

(C) By flow cytometry, approximately 4% of *Nes-GFP*-positive cells recombined (that is, were both green and red).

(D–H) This specific *Nes-CreERT* transgenic line recombined in all typical *Nes-GFP* populations, including perivascular cells immediately inferior to the growth plate (D), in periarteriolar cells (E), and in perisinusoidal *Nes-GFP*-positive cells (red arrows, F–H). The only osteochondral lineage tracing found were isolated osteocytes throughout the diaphyseal bone (H, white arrow).

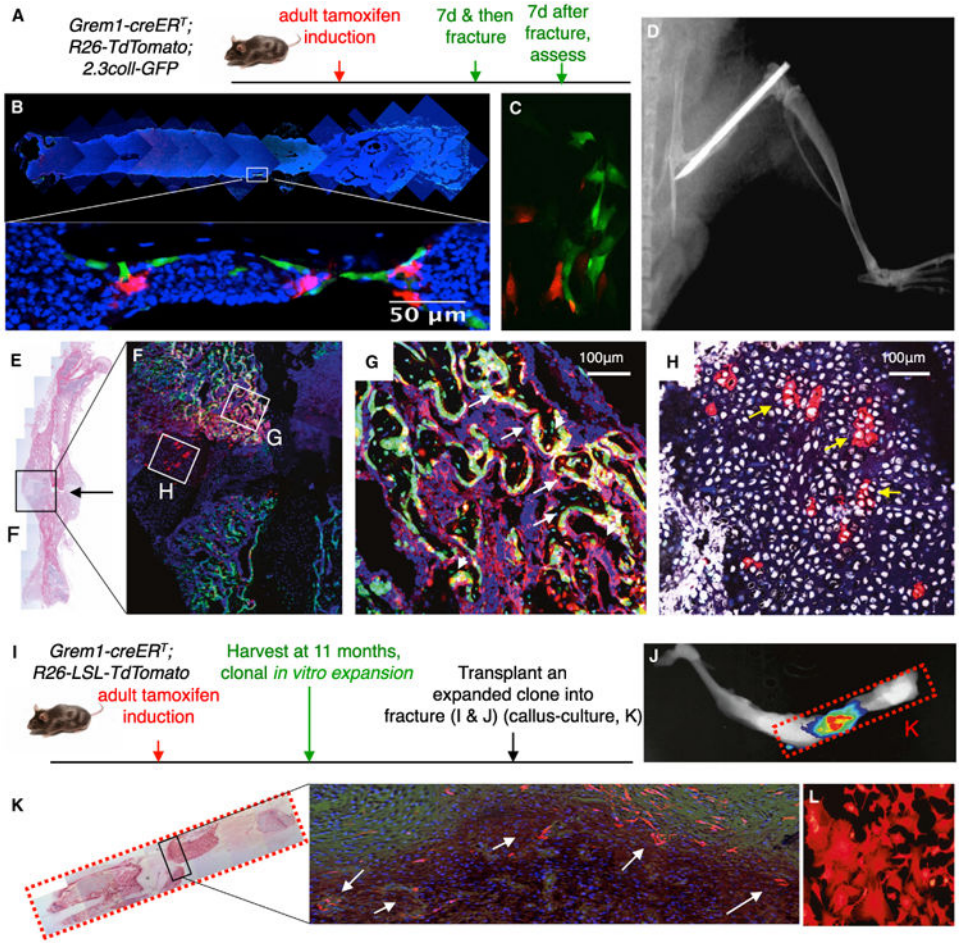

Figure 5. Adult *Grem1* Cells, Both Endogenous and Transplanted, Differentiate into Osteochondral Fracture Callus

(A) Protocol.

(B and C) *Grem1-creER^T;R26-LSL-TdTomato;2.3colGFP* mice adult induction: *Grem1*$^+$ (red) cells were not osteoblasts (green) but were adjacent to each other in situ (B) and during the first week of adherent bone marrow stromal culture (C).

(D) is an X-ray of the femoral osteotomy and internal fixation of the bone.

(E) and (F) show the serial histology and fluorescent microscopy sections from the resulting fracture callus after the osteotomy.

(G) and (H) are magnified from areas shown in (F). *Grem1*$^+$ cells (red) stream into the fracture site and differentiate into either osteoblasts (G, yellow cells, white arrows) or Sox9$^+$ (white, nuclear stain) chondrocytes (yellow arrows) (H).

(I) A *Grem1*$^+$ clone, after adult induction, was expanded in vitro. An osteotomy with internal fixation was performed in wild-type mice, at which point 500 × 10^6 clonal cells (red) were irrigated into the surgical field. Seven days later, the *Grem1* clone had engrafted (J), the site of injury was identified by TdTomato fluorescence imaging, and recombined cells (fluorescent red) differentiated into osteoblastic cells (K) (alkaline phosphatase positive cells, red-brown, white arrows) in the callus (sequential fluorescence microscopy and ALP staining performed on the same slide).

(L) Callus culture was performed, and the recombined *Grem1* cells were easily recovered in vitro and serially transplanted into a secondary fracture (Figure S4E).

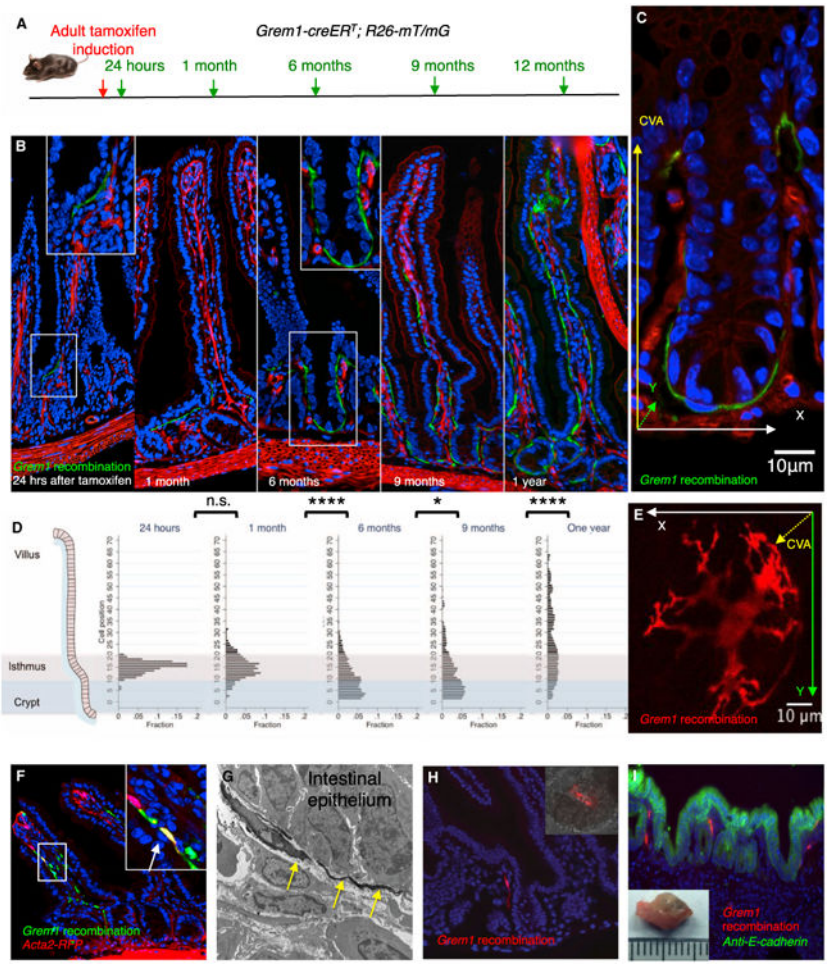

Figure 6. *Grem1* Expression Identifies iRSCs

(A) Protocol.

(B and C) *Grem1-creER^T;R26-mT/mG* adult induction identifies rare, single cells at the junction of the crypt and villus in the small intestine (green = *Grem1-creER^{T+}*, red = *Grem1-creER^T*-negative). Over 1 year, *Grem1$^+$* cells expand to renew the entire periepithelial mesenchymal sheath. By 6 months, they are immediately beneath the intestinal stem cells at the crypt base (B and C). Axes are provided to indicate the longitudinal and circumferential axes (x and y), and "CVA" to designate the crypt-villus, or radial, axis.

(D) The mesenchymal expansion was plotted relative to the adjacent epithelial position; 20 well-orientated crypt-villus columns were quantified per mouse. n = 3– 5 mice at each time point; Kruskal-Wallis analysis ($p < 0.0001$) and post-hoc pairwise Mann-Whitney tests, corrected for multiple comparisons, revealed significant differences (****$p \leq 0.0001$, *$p \leq 0.05$).

(E) The sheath was comprised of a reticulated population of stellate cells with long processes that encircled the entire intestinal gland. This cell encapsulated the very base of the intestinal crypt, similar to the position of the cell identified in (C).

(F) The *Grem1$^+$* population self-renewed and was multipotent, generating both *Acta2* positive (yellow cell, white arrow) and negative fibroblastic lineages.

(G) Transmission electron microscopy: the *Grem1* lineage (yellow arrows) is immediately beneath the epithelial cells.

(H) Tissue engineering: representative images from n = 8 small-intestinal organoid unit transplants. Small intestines were harvested from 3-week-old, tamoxifen-induced donor mice. In the donor intestines, prior to harvest, there were single *Grem1*$^{+}$ cells (red) near the isthmus of the intestinal gland. After digestion of the donor intestines into organoid units, rare *Grem1*$^{+}$ mesenchymal cells (red) were found within individual organoid units (inset).

(I) Four weeks after transplantation, TESIs develop, with the periepithelial mesenchymal sheath recapitulated from the donor *Grem1*$^{+}$ cells (red). E-cadherin staining (green) was used to identify the epithelium.

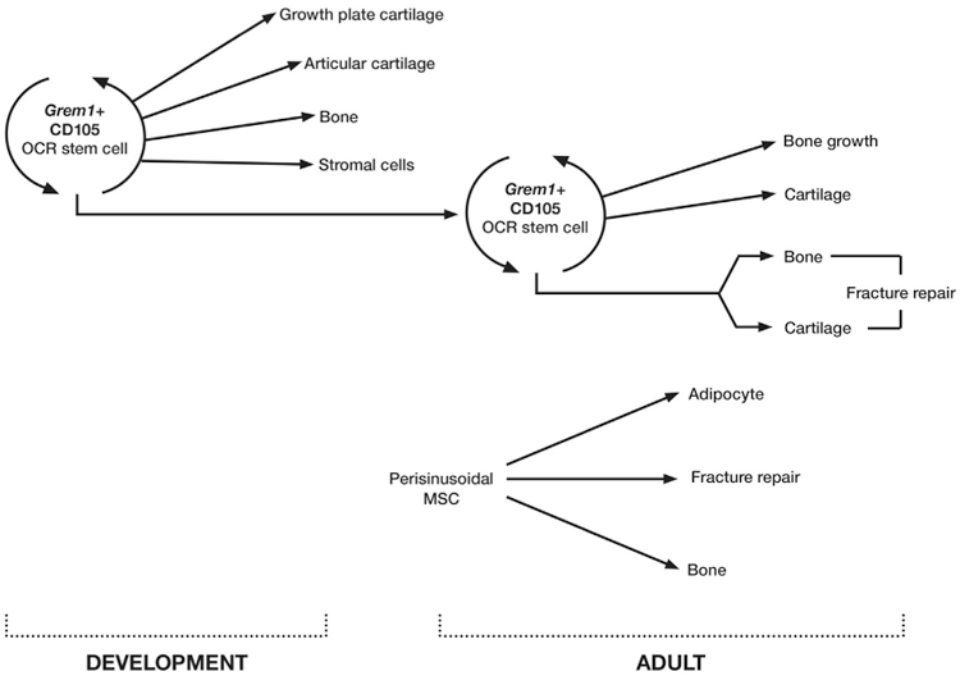

Figure 7. A Model in which the OCR Stem Cell and the Perisinusoidal MSC Make a Complementary Contribution to Skeletal Development, Adult Homeostasis, and Repair